Studies of Aggregation Effects on SO_x Removal by Limestone Powder

Yoshio Kobayashi
Technical Development Headquarters, Hitachi Zosen Corp., Osaka 554, Japan

To analyze effects of aggregation in powder/gas reactions quantitatively, particle packing models were applied to aggregate structures, and theoretical equations of the reaction rate, the reaction-equivalent particle radius, the acid gas concentration exponent and the particle radius exponent were deduced. While confirming the validity of these equations by comparing experimental values (data on SO_x removal in aerosol reactions and stationary reactions) to these equations, other experimental data were analyzed using these equations. The results show that: the dependency of lime conversion on the particle size decreases sharply as the aggregation of particles in the aerosol advances; injecting limestone powder into the furnaces, using a high rate dispersion nozzle, reduces the degree of aggregation and elevates the lime conversion; and in thermobalance analysis of SO_x/limestone reactions, bulk limestone powder behaves like a single giant particle, and the diffusion process inside the aggregates is controlling. It is concluded that hexagonal closest packing is the optimal packing model for the particles constituting aggregates in aerosol.

Introduction

In Japan and other developed countries, wet flue-gas desulfurization has often been used to remove SO_x, a cause of acid rain. In the search for countermeasures against acid rain that have world-wide applicability, however, public attention has been paid to dry flue-gas desulfurization, which is economically cheaper, although SO_x removal is less complete than in the wet technique. This article will deal with a method of dry flue-gas desulfurization, in which SO_x is removed by injecting limestone powder into furnaces and thus inducing the formation of aerosols of fine lime particles. Since first reported by Wickert (1963) about 30 years ago, this technique has been studied by numerous investigators.

To date, Borgwardt (1985, 1989a,b), Borgwardt and Bruce (1986), and Borgwardt et al. (1986) have made a number of basic studies of the reaction between fine lime powder and SO_2. In those studies, the relationship of reaction temperatures and residence times with CaO reactivity has been investigated in detail. However, all of these past basic studies pertained to reactions in stationary conditions. Few articles have ever dealt with the principles of these reactions in the form of aerosols.

Because reactions in the form of aerosols, which behave in a complex manner, are difficult to predict on the basis of reaction data obtained in stationary conditions, no noteworthy progress has been achieved in the development of valid techniques for dry flue-gas desulfurization. To facilitate the development of dry techniques, it seems essential to establish a basic reaction theory for aerosol conditions.

By applying an unreacted core model (a model well known for its ability to accurately represent solid/gas reaction rates) to aerosol reaction systems, the author previously deduced theoretical equations concerning reaction rates of aerosols, that is, of nonaggregated primary particles (Kobayashi, 1993). The validity of these equations was then tested by comparing the data obtained from experiments on aerosol reactions (Kobayashi, 1993). Using those equations, the author then attempted to clarify the cause of the low lime conversion (about 10–20%) of the dry flue-gas desulfurization using lime particle aerosol, which is the most serious problem with this dry method (Kobayashi, 1993). That theoretical analysis revealed that the particle radius exponent (m_2), which represents the dependency of lime conversion on particle sizes (cf. Eq. 24), is equal to 0.85–0.97. This finding differed from the previous experimental values of $m_2 = 0.25$–0.33 reported by numerous investigators, who say that the lime conversion is not substantially improved even when the lime particle size is reduced. To explain these theoretical and experimental discrepancies, the author had pointed out that the tendency of primary par-

ticles to aggregate into coarse particles becomes more marked as the size of primary particles decreases, and that therefore the SO_x-removing efficiency in an aerosol environment will not be elevated satisfactorily even when the particle size is reduced (Kobayashi, 1993).

The present article reports the author's subsequent attempt to make a quantitative evaluation of the effects of aggregation. First, the author calculated the effects of aggregation on the mass-transfer rate, based on the assumption that the aggregates are composed of packed primary particles of the same particle size. The results of this calculation were then applied to the theoretical equations for aerosol reaction rates that the author previously reported (Kobayashi, 1993). By this means, the author deduced theoretical reaction rate equations for aggregates. The validity of these equations was subsequently confirmed by comparing the equations with the data from experiments concerning aerosol reactions, as well as experiments concerning stationary reactions. Stationary reactions represent a particular case of aerosol reactions in which the stoichiometric ratio (SR) of limestone to SO_x is extremely small and the R/r (degree of aggregation) is extremely large. In this way, the effects of aggregation on lime reactivity was quantitatively analyzed, using the author's theoretical equations.

Theoretical Consideration of Effects of Aggregation in Powder/Gas Reaction Systems

Packing models for aggregated particles

The aggregating effect in powder/gas systems is the effect produced by restriction of mass transfer to the surfaces of inner primary particles due to aggregation of primary particles. This means that when the mass transfer to primary particles, which constitute aggregates, occurs through the surface of the aggregates, the mass-transfer resistance in the gas layer (on the surface of primary particles constituting the aggregates) is apparently increased because the external surface area of primary particles inside the aggregates is much greater than the void area of the aggregate's surface. To calculate the magnitude of this resistance, it is indispensable to determine the relationship between the void fraction on the aggregate's surface and the packing fraction inside the aggregate.

Before a powder packing model can be designated, it is necessary to outline the structure of powders.

Gotoh (1983) studied the packing fraction and fluidity of powders and liquids and found that the packing structure of powders is similar to that of liquids. According to textbooks of physical chemistry, liquids are structurally composed of random groups of microsegments (microcrystals) made up of orderly arranged molecules or atoms. Fluidity is attributable to such structural features.

In view of this finding, it seems likely that bulk powders are composed of random groups of aggregates (secondary particles) made up of orderly packed primary particles. It is also likely that in aerosols, such aggregates (secondary particles) are floating in gas.

The size of an aggregate is determined by the balance between the shearing stress that the aggregate receives from outside and the attraction force among primary particles. In other words, it may be said that the aggregate in aerosol, whose size is determined by the magnitude of the turbulence of gas flow during aerosol genesis, has an ordered packing structure, while bulk powders, which are stationary, are macroscopically characterized by random packing structure.

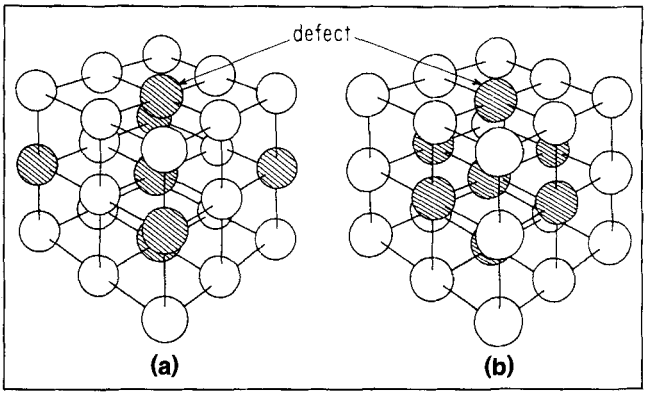

Figure 1. Random packing models of aggregate.
(a) Simple cubic lattice with defect; (b) simple cubic lattice with defect.

The validity of the hypothesis that an aggregate in aerosol has an ordered packing structure will be tested later using experimental data in the section on aerosol reaction experiments by using an ordinary injection nozzle.

To determine the relationship between the void fraction on the aggregate surface and the packing fraction inside the aggregate for every possible density of packing, ranging from low-density random packing to high-density ordered packing, the author imagined four models of ordered packing (hexagonal closest packing, cubic closest packing, orthorhombic lattice, and simple cubic lattice) and two models of random packing in Figure 1. On the basis of a hypothesis that uniform-size spheres are arranged in contact with each other at the lattice points of these models, the superficial packing fraction (at surface β) and the bulk packing fraction (in volume α) are calculated for each model, considering the geometrical structures of these models. The results of these cal-

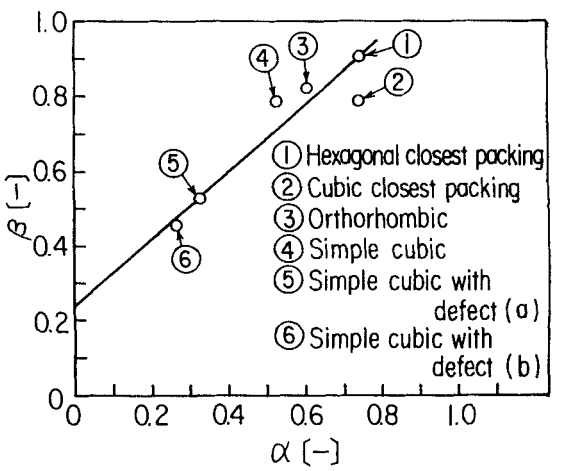

Figure 2. Relationship between packing fraction in volume (α) and in surface (β) in various packing models.

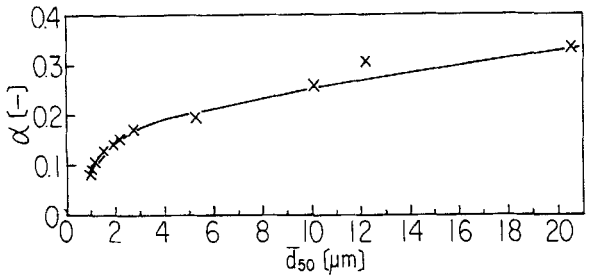

Figure 3. Relationship between mean particle diameter ($\bar{d}_{50}$) and packing fraction in volume (α) in softly static state of powder.

culations are approximately on a single line, as shown in Figure 2.

Although the packing fraction of bulk powder varied greatly depending on the particle size and the manner of packing, the relationship between the mean particle diameter ($\hat{d}_{50}$) and the packing fraction (α) of limestone powder, as measured using the method prescribed in the Japanese Industrial Standard (JIS K5101), that is, setting the powder gently, is shown in Figure 3 (Nitto Funka Kogyo). In subsequent simulations using the random packing model, the relationship among α, β, and $\hat{d}_{50}$, as shown in Figures 2 and 3, was used.

If an aggregate is assumed to have the form of a sphere, the number of primary particles constituting the aggregate (n) and the number of primary particles constituting the superficial layers of the aggregate (n_1) are expressed by Eqs. 1 and 2, respectively:

$$n = \alpha(R/r)^3 \tag{1}$$

$$n_1 = 4\beta(R/r - 1)^2 \tag{2}$$

where R/r is the ratio of the aggregate's radius to the primary particle's radius. This ratio indicates the degree of aggregation and will be referred to in this article as the degree of aggregation or the geometrical particle-size ratio.

Expansion of the overall reaction rate equation to aggregated particle systems

The author previously reported the reaction rate equations of an integral form for aerosol reaction systems obtained by applying unreacted core models to the aerosol reaction system composed of primary particles (Kobayashi, 1993).

A case where gas layer diffusion is controlling:

$$F_1 = \frac{(C_{f_0} - C_{f_e})D_m \cdot \theta}{\rho \cdot r^2} = -\frac{1}{3 \cdot SR}\ln(1-\eta) \tag{3}$$

A case where reaction product layer diffusion is controlling:

$$F_2 = \frac{(C_{f_0} - C_{f_e})D_e \cdot \theta}{\rho r^2} = (1-f)^{-1/3} + 1/3\ln(1-f) - 1 \qquad (SR = 1) \tag{4}$$

$$F_2 = \frac{1}{\epsilon^{1/3} \cdot SR}\left\{\frac{1}{6}(1+2\epsilon^{1/3})\ln(1-\eta) - \frac{1}{2}\ln\frac{\epsilon^{1/3} - (1-f)^{1/3}}{\epsilon^{1/3} - 1} - \frac{1}{\sqrt{3}}\left[\tan^{-1}\frac{\epsilon^{1/3} + 2(1-f)^{1/3}}{\sqrt{3}\,\epsilon^{1/3}} - \tan^{-1}\frac{\epsilon^{1/3} + 2}{\sqrt{3}\,\epsilon^{1/3}}\right]\right\} \qquad (SR \neq 1) \tag{5}$$

A case where chemical reaction is controlling:

$$F_3 = \frac{(C_{f_0} - C_{f_e})k_c \cdot \theta}{\rho \cdot r} = \frac{1}{2}[(1-f)^{-2/3} - 1] \qquad (SR = 1) \tag{6}$$

$$= \frac{1}{\epsilon^{2/3} \cdot SR}\left[\frac{1}{3}(1+\epsilon^{1/3})\,\ell n(1-\eta) - \ln\frac{\epsilon^{1/3} - (1-f)^{1/3}}{\epsilon^{1/3} - 1}\right] - \frac{F_2}{\epsilon^{1/3}} \qquad (SR \neq 1) \tag{7}$$

Overall reaction rate equation:

$$F_0 = \frac{(C_{f_0} - C_{f_e})D_e \cdot \theta}{\rho \cdot r^2} = \frac{D_e}{k_f \cdot r}F_1 + F_2 + \frac{D_e}{k_c \cdot r}F_3 \tag{8}$$

where

C_{f_0} = concentration of gas in inlet, mol·m^{-3}
C_{f_e} = equilibrium concentration of gas, mol·m^{-3}
D_e = effective diffusivity in reaction product layer, m^2·s^{-1}
D_m = molecular diffusivity of SO_2 in combustion gas, m^2·s^{-1}
f = lime conversion
k_c = chemical reaction rate constant, m·s^{-1}
r = particle radius of limestone powder, m
SR = stoichiometric ratio of limestone to SO_x ($SR \cdot f = \eta$)
ϵ = calculation operator given in $\epsilon = 1 - 1/SR$
η = SO_x conversion
θ = reaction time, s
ρ = molal density of limestone, mol·m^{-3}

In the aggregated particle reaction systems, the magnitude of mass transfer per unit surface area may vary among individual primary particles. To simplify the calculation of the magnitude of mass transfer in the aggregated particle system, primary particles are divided into two groups: primary particles exposed on the surface of the aggregate and primary particles incorporated into the aggregate. The latter includes the inside-facing plane of the primary particles constituting the superficial layers of aggregates. For each of these two groups of primary particles, the author calculates the apparent mass-transfer coefficient in the gas layer and the overall reaction rate equation. A weighted average of these overall reaction rate equations is then obtained as an overall reaction rate equation for the aggregated particle reaction system.

The mass transfer toward the primary particles constituting the aggregate occurs through the surface of the aggregate. Since the surface area of the primary particles constituting an aggregate is greater than the external surface area of the aggregate, the mass transfer toward the surface of the primary particles constituting an aggregate is restricted, as described

in the previous section. This means that since the diffusional flux toward the surface of primary particles within an aggregate is equal to the diffusional flux toward the surface of the aggregate, the diffusional flux per unit surface area of primary particles constituting an aggregate decreases, depending on the ratio of aggregate's surface area to the primary particles' surface area.

The magnitude of the decrease in the diffusional flux per unit surface area of primary particles can be obtained from calculations based on the primary particle surface area, the external surface area of an aggregate, and Eqs. 1 and 2.

The magnitude of the decrease on the surface of an aggregate can be obtained as follows: (The packing area on the aggregate's surface)/(The primary particle's external surface area exposed on the aggregate's surface)

$$= \frac{4\pi R^2\beta}{4\pi r^2 \cdot 1/2n_1} = \frac{1}{2(1-r/R)^2} \tag{9}$$

The magnitude of the decrease inside an aggregate can be obtained as follows: (The void area on the aggregate's surface)/(The primary particle's external surface area incorporated into the aggregate's inner part)

$$= \frac{4\pi R^2(1-\beta)}{4\pi r^2(n-1/2n_1)} = \frac{(1-\beta)(r/R)}{\alpha - 2\beta(r/R)(1-r/R)^2} \tag{10}$$

In other words, it may be said that aggregation of primary particles leads to apparent reduction in the mass-transfer coefficient by these degrees. The apparent mass-transfer coefficient in the gas layer of aggregate constituting primary particles can be therefore expressed as follows.

The coefficient on the aggregate surface:

$$k'_{f_0} = \frac{1}{2(1-r/R)^2} K_f \tag{11}$$

The coefficient inside the aggregate:

$$k'_{f_1} = \frac{(1-\beta)(r/R)}{\alpha - 2\beta(r/R)(1-r/R)^2} \cdot K_f \tag{12}$$

In aerosol reaction systems, the relative linear velocity between gas and particles is approximately equal to zero. For this reason, the gas layer is adequately thick. If the distance between two neighboring particles in such systems is denoted by L, the actual thickness of the gas layer can be expressed as $L/2$, and the mass-transfer coefficient in the gas layer of aerosols can be expressed by Eqs. 13 and 14. How these equations were deduced is shown in Appendix A:

$$k_f = \frac{D_m}{r(1-2r/L)} \fallingdotseq \frac{D_m}{r} \quad \text{(for single particle in aerosol)} \tag{13}$$

$$K_f = \frac{D_m}{R(1-2R/L)} \fallingdotseq \frac{D_m}{R} \quad \text{(for aggregate in aerosol)} \tag{14}$$

Overall reaction rate equations for individual particles can be obtained from Eqs. 11 and 12 (equations pertaining to the mass-transfer coefficient in gas layer) and Eq. 8. If these equations are subjected to weighted averaging, an overall reaction rate equation for an aggregate system can be obtained, as shown below:

$$\left(\frac{D_e}{k'_{f_0} \cdot r}F_1 + F_2 + \frac{D_e}{k_c \cdot r}F_3\right) \cdot \frac{1}{2} \cdot \frac{n_1}{n} + \left(\frac{D_e}{k'_{f_1} \cdot r}F_1 + F_2 + \frac{D_e}{k_c \cdot r}F_3\right)\left(1 - \frac{1}{2} \cdot \frac{n_1}{n}\right) = AF_1 + F_2 + \frac{D_e}{k_c \cdot r}F_3 = \frac{(C_{f_0} - C_{f_e})D_e \cdot \theta}{\rho \cdot r^2} = F_0, \tag{15}$$

where A is expressed by Eq. 16 (taking into account Eq. 14):

$$A = \frac{D_e}{D_m} \cdot \frac{1}{1-\beta} \cdot \left[\frac{4\beta}{\alpha} \cdot \left(1 - \frac{r}{R}\right)^4 + \alpha\left(\frac{R}{r}\right)^2 - 4\beta\left(\frac{R}{r}\right)\left(1 - \frac{r}{R}\right)^2\right] \tag{16}$$

where F_1, F_2, and F_3 correspond to Eqs. 3 through 7. If the A in Eq. 15 is deemed as being equal to D_e/D_m, an overall reaction rate equation for an aerosol system composed of primary particles can be obtained.

Rate-controlling step and the equivalent radius to reaction in aggregated particle reaction systems

The author has previously demonstrated that the diffusion processes within the layer of reaction products are the rate-controlling step for aerosols composed of primary particles (Kobayashi, 1993).

As the particle size decreases and aggregation progresses, the mass transfer toward the interior of the aggregate is restricted. As a result, resistance against diffusion within the aggregate appears to be predominant, and the aggregate begins to behave as if it were a single particle (a primary particle). However, since the aggregate has large voids within it, it is more reactive than a single particle (primary particle) of the same geometrical particle size. Here, the author assumes an imaginary primary particle that is as reactive as an aggregate with a radius of R. The radius of this particle is defined as the equivalent radius to reaction (R'). Discussion of the imaginary primary particles follows.

The overall reaction rate equation for primary particles (Eq. 8) is modified for R' to yield Eq. 8′:

$$\frac{D_e}{D_m}F_1 + F_2 + \frac{D_e}{k_c \cdot R'}F_3 = \frac{(C_{f_0} - C_{f_e})D_e \cdot \theta}{\rho' R'^2} = F' \tag{8'}$$

where ρ' denotes the molal density of the aggregate. From Eqs. 8′ and 15, an equation expressing the reaction-equivalent particle radius ratio (R'/r) can be obtained. Since ρ'/ρ corresponds to the packing fraction in volume (α), the R'/r can be expressed by Eq. 17:

$$\frac{R'}{r}=\frac{-\frac{D_e}{k_c\cdot r}\cdot F_3+\left[\left(\frac{D_e}{k_c\cdot r}\cdot F_3\right)^2+\frac{4}{\alpha}\cdot\left(\frac{D_e}{D_m}\cdot F_1+F_2\right)F_0\right]^{1/2}}{2\left(\frac{D_e}{D_m}\cdot F_1+F_2\right)} \tag{17}$$

This equation indicates the relationship of the lime conversion (f) and the degree of aggregation (R/r) with the reaction-equivalent particle radius ratio (R'/r). Since R'/r is a function of f, the R'/r value at a given f should be evaluated as a mean of 0 through f expressed by Eq. 18:

$$(\bar{R}'/r)=(1/f)\cdot\int_0^f(R'/r)\,df \tag{18}$$

Here, $\bar{R}'/r$ is called the effective reaction-equivalent radius ratio, and $\bar{R}'$ is called the effective reaction-equivalent radius. The order of magnitude of these three values is $R/r > \bar{R}'/r > R'/r$ (cf. Figure 7).

If Eq. 15 is normalized by dividing it by F_0, Eq. 19 can be obtained:

$$A\frac{F_1}{F_0}+\frac{F_2}{F_0}+\frac{D_e}{k_c\cdot r}\cdot\frac{F_3}{F_0}=1 \tag{19}$$

The first term of this equation indicates the contribution of the diffusion processes in the gas layer. The second term indicates the contribution of the diffusion processes in the layer of reaction products. The third indicates the contribution of chemical reaction processes.

Theoretical equations for the acid gas concentration exponent in aerosol systems composed of aggregated lime particles

The influence of acid gas concentrations on the lime conversion in aerosol systems composed of primary particles of lime has already been described elsewhere by the author (Kobayashi, 1993). This section will describe this influence in aerosol systems composed of aggregated particles.

If equilibrium gas concentration (C_{fe}), which is very low under ordinary reaction conditions, is ignored, the contribution of acid gas concentrations to lime conversion is given by

$$f=g_1[C_{f_0}]^{m_1} \tag{20}$$

where g_1 is a proportional constant. If m_1 is defined as the acid gas concentration exponent, it can be expressed by

$$m_1=\frac{d\ln f}{d\ln C_{f_0}}=\frac{C_{f_0}}{f}\cdot\frac{df}{dC_{f_0}} \tag{21}$$

where m_1 can be obtained by calculating df/dC_{f_0} using Eq. 15.

When $SR=1$ and R/r (degree of aggregation) $=1$, Eq. 22 is obtained, since A (in Eq. 15) $=D_e/D_m$:

$$m_1=\frac{F_0}{f}\cdot\frac{3(1-f)}{(1-f)^{-1/3}+D_e/D_m-1+D_e/(k_c\cdot r)(1-f)^{-2/3}} \tag{22}$$

When the SR is equal to 1 but the R/r is larger than 1, Eq. 23 is obtained.

$$m_1=\frac{F_0}{f}\cdot\frac{3(1-f)}{(1-f)^{-1/3}+A-1+D_e/(k_c\cdot r)(1-f)^{-2/3}} \tag{23}$$

Theoretical equations for the particle radius exponent in aerosol systems composed of aggregated lime particles

The influence of particle sizes on the lime conversion in aerosol systems composed of primary particles of lime has already been described by the author (Kobayashi, 1993). This section will describe this influence in aerosol systems composed of aggregated particles.

The contribution of particle sizes to lime conversion is

$$f=g_2\left[\frac{1}{r}\right]^{m_2} \tag{24}$$

where g_2 is a proportional constant. If m_2 is defined as the particle radius exponent, it is given by Eq. 25.

$$m_2=\frac{d\ln f}{d\ln(1/r)}=-\frac{r}{f}\cdot\frac{df}{dr} \tag{25}$$

This exponent can also be expressed by Eq. 26, considering the relationship of this exponent with the acid gas concentration exponent given in Eq. 21.

$$m_2=-\frac{r}{C_{f_0}}\frac{dC_{f_0}}{dr}\cdot m_1 \tag{26}$$

where m_2 can be obtained by calculating dC_{f_0}/dr using Eq. 15 as follows:

$$m_2=-\left(2+r\cdot\frac{dA}{dr}\cdot\frac{F_1}{F_0}-\frac{De}{k_c\cdot r}\cdot\frac{F_3}{F_0}\right)m_1 \tag{27}$$

Equation 27 is the basic equation for m_2.

When $SR=1$ and $R/r=1$, the following relationship is obtained, because the A is equal to D_e/D_m:

$$m_2=-\left(2-\frac{D_e}{k_c\cdot r}\cdot\frac{F_3}{F_0}\right)m_1 \tag{28}$$

When $SR=1$ but $R/r>1$, Eq. 27 can be converted into Eq. 29 by calculating dA/dr using Eq. 16:

$$m_2=-\left[2-\frac{D_e}{k_c\cdot r}\cdot\frac{F_3}{F_0}+\frac{D_e}{D_m}\cdot\frac{F_1}{F_0}\cdot\frac{1}{\beta-1}\times\left\{\frac{16\beta}{\alpha}\left(1-\frac{r}{R}\right)^3\left(\frac{r}{R}\right)+2\alpha\left(\frac{R}{r}\right)^2-4\beta\cdot\left(1-\left(\frac{r}{R}\right)^2\right)\left(\frac{R}{r}\right)\right\}\right]m_1 \tag{29}$$

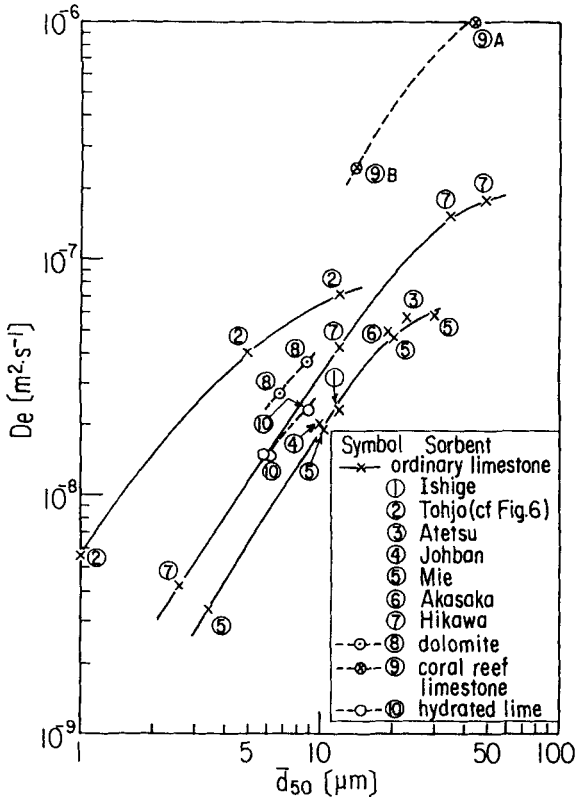

Figure 4. Relationship between mean particle diameter ($\bar{d}_{50}$) and effective diffusivity in reaction product layer (D_e) calculated from experimental data.

Designation of D_e, D_m, and k_c Values for Simulation in Theoretical Equations

Calculation of the D_e value from the experimental data and designation of the D_e value

The D_e value is estimated by analyzing the data concerning SO_x removal using aerosols of limestone powder, reported by Ishihara et al. (1968, 1975) and Ishihara and Hukuzawa (1970). The author calculated the D_e value by applying their experimental data to Eq. 4. Figure 4 shows the results of this calculation. Table 1 shows the chemical composition of the sorbents used for SO_x removal in that experiment. The reaction time was set at 3 s in this calculation.

Although the D_e value is expected to be a physical property and hence theoretically to be independent of particle size, a correlation was noted in the actual fact between this D_e value calculated by the preceding method and the particle size as shown in Figure 4. This is probably due to the influence of aggregation. If the particle size becomes too large to allow aggregation, the D_e value must reach the original level of this physical property.

Of the limestones produced in various mines in Japan, the limestones from Ishige, Atetsu, Johban, Mie, and Akasaka are approximately on a single curve, indicating the relationship between the D_e value and the mean particle diameter ($\bar{d}_{50}$). The curve for Hikawa's limestone is shifted upwards from this curve, although it has the same gradient as that for the limestones from the just mentioned mines. The curve for

Table 1. Chemical Composition of Various Sorbents for SO_x Removal

Mining District	Chemical Composition (%)					MgO/CaO (Molal Ratio)
	CaO	MgO	Fe_2O_3	SiO_3	Al_2O_3	
Ordinary limestone						
Ishige	55.55	0.0	0.03	0.08	0.27	0.00
Tohjo	55.10	0.65	0.02	0.14	0.03	0.017
Atetsu	53.70	0.91	0.42	0.26	0.12	0.024
Johban	54.33	1.17	0.08	0.44	0.16	0.030
Mie	53.20	1.37	0.63	0.34	0.52	0.036
Akasaka	51.45	1.82	0.58	0.60	0.28	0.050
Hikawa	50.00	5.69	0.53	4.00	1.48	0.159
Dolomite						
Kuzuu	37.05	15.90	0.28	1.40	0.68	0.601
Coral reef limestone						
Tokunoshima	51.80	1.81	0.28	1.34	0.18	0.049
Tokunoshima	49.50	0.00	0.40	7.12	1.45	0.00
Hydrated lime						
Kuzuu	68.29	2.82	0.13	2.64	0.39	0.049

Kuzuu's dolomite is an even further upwards shifted curve from that of Hikawa's limestone.

Of the components of the sorbents used for SO_x removal, Fe_2O_3, and MgO seem to promote desulfurizing reactions. Fe_2O_3 accelerates the conversion of SO_2 to SO_3, which favorably affects the desulfurizing reactions at lower temperatures and prolongs the effective reaction time. MgO, which is not reactive with SO_x, seems to indirectly enhance the desulfurizing reactions by suppressing obstruction of micropores.

The percentage of the sorbents (limestone or dolomite) occupied by Fe_2O_3 did not differ greatly among different mines (0.53% for Hikawa's limestone, 0.28% for Kuzuu's dolomite, and 0.03–0.63% for other mines' limestones). The percentage occupied by MgO was 5.7% for Hikawa's limestone and 15.9% for Kuzuu's dolomite, but it was lower (0–1.8%) for other mines' limestones. The D_e value went from highest to lowest in the following order: Kuzuu > Hikawa > Ishige, Atetsu, Johban, Mie, and Akasaka. This order was identical with the order of the MgO percentage (or the MgO/CaO ratio). Therefore, the high D_e value for Hikawa's limestone seems to be attributable to MgO.

Figure 4 also shows the D_e values when high-rate dispersion nozzles (cf. Figure 6) were used. As noted in this figure, the D_e values using the high-rate nozzle were considerably higher than the values using an ordinary nozzle and the gradient of the curve was smaller, when the particle size was below 10 μm. When the particle size was over 30–50 μm, the D_e value tended to converge at about 10^{-7} $m^2 \cdot s^{-1}$, similar to the tendency shown by Ishige's, Atetsu's, Johban's, Mie's and Akasaka's limestones injected using ordinary nozzle.

The finding that the D_e value converged at 10^{-7} $m^2 \cdot s^{-1}$ when $\bar{d}_{50}$ was over 30–50 μm is probably explained by the low content of Fe_2O_3 and MgO in the Tohjo's limestone (used in this experiment), similar to Ishige's, Atetsu's, Johban's, Mie's, and Akasaka's limestones. The finding that the D_e value of particles smaller than 10 μm was higher for Tohjo's limestone than for Ishige's and other mines' limestones can be interpreted as clearly indicating the dispersing effect of the high-rate nozzle. That is, the gradient of the curve indicating the relationship between D_e value and $\bar{d}_{50}$ represents the dispersing efficiency of the nozzle. The smaller the gradi-

ent, the higher the dispersing efficiency. Furthermore, the magnitude of the converged D_e value for $\bar{d}_{50} \to \infty$ is determined by the chemical composition and porosity of the sorbent. Therefore on the basis of the data shown in Figure 4, it seems reasonable to regard the true D_e value of ordinary limestone, which does not contain much MgO or Fe_2O_3, as $1.0 \times 10^{-7}\ m^2 \cdot s^{-1}$.

To analyze this issue from another viewpoint, the author calculated the micropore size by applying this D_e value to the Knudsen's diffusion equation, shown below:

$$D_e \doteqdot 3.067a(T/M)^{1/2} \tag{30}$$

When the D_e value equals $1.0 \times 10^{-7}\ m^2 \cdot s^{-1}$, a was equal to 2.3×10^{-10}m. Therefore, the micropore size was 4.6 Å.

The superficial $CaSO_4$ layer of the sorbents used for SO_x removal is formed by the following steps:

$$CaCO_3 \to CaO \to CaSO_4$$

Considering that the weight of the sorbents has increased by 36% at the end of these steps, without being accompanied by a corresponding increase in the volume of the sorbents, the micropore size may be estimated at about 1 Å. When compared with this value, the micropore size (4.6 Å) mentioned earlier appears to be somewhat large, but still to be within a reasonable range. Therefore, in subsequent simulations, *the D_e value was set at $10^{-7}\ m^2 \cdot s^{-1}$.*

The D_e value of Tokunoshima's limestone (a coral reef), which is well known to be highly porous, was 9–10 times that of ordinary limestone. This seems to reflect the porous nature of Tokunoshima's limestone. The specific surface area of the limestones used for this experiment was as follows: Tokunoshima limestone, 5.6–6.8 m^2/g; Mie limestone, 1.1 m^2/g; Johban limestone, 2.0 m^2/g. The D_e value of the slaked lime was close to that of Hikawa's limestone.

Designation of the value of D_m

Using the equation of Gilliland (1934), the author calculated the molecular diffusivity (D_m) of SO_2 in gas burned at 1,000°C. This calculation yielded a D_m value of 0.952×10^{-4} $m^2 \cdot s^{-1}$. In subsequent simulations, therefore, *the D_m value was set at $1.0 \times 10^{-4}\ m^2 \cdot s^{-1}$.*

Designation of the value of k_c

In analyses of the reaction rates using Thiele's modulus, Ishihara et al. inferred that the diffusive resistance in the reaction product layer would be equal to the chemical reaction resistance in the initial reaction phases of limestone powder of a size between about 5 and 20 microns (Ishihara et al., 1975; Ishihara and Hukuzawa, 1970, 1975a,b).

Furthermore, if the linear segment (including its origin of the coordinates) of the f vs. θ curve in Ishihara's article is regarded as representing the initial phases of the reaction, the lime conversion in the initial phases (f) is estimated to be less than 0.025–0.05. Bearing these reports in mind, the author estimated the value of k_c (chemical reaction rate constant) in the following steps. Considering that the resistance during chemical reaction processes is equal to that during diffusion within the layers of reaction products when ($\bar{d}_{50}$) is equal to 10 μm and f is equal to 0.025, the second term of the left side of Eq. 19 is equal to the third term of the same. Thus Eq. 31 is obtained:

$$k_c = \frac{D_e}{r} \cdot \frac{F_3}{F_2}. \tag{31}$$

Substitution of $10^{-7} m^2 \cdot s^{-1}$ for D_e, 5.0×10^{-6} m for r, 3.57×10^{-5} for F_2, and 8.51×10^{-3} for F_3 yields a k_c value of 4.77 $m \cdot s^{-1}$. Therefore, *the K_c value was set at 5.0 $m \cdot s^{-1}$.*

Experimental Validation of the Reaction Theory of Aggregated Particle Systems

Aerosol reaction experiments by using an ordinary injection nozzle

Ishihara et al. (1967, 1975) carried out some aerosol reaction experiments with varying particles sizes of limestone, and reported some experimental data concerning the relationship between the mean particle diameter ($\bar{d}_{50}$) and the lime conversion (f). Using their data, the author tested the validity of the theory presented in this article.

According to the present theory, the relationship between the mean particle diameter ($\bar{d}_{50}$) and the degree of aggregation (R/r) at two experimental points in an aerosol can be calculated from the experimental data concerning the relationship between $\bar{d}_{50}$ and f at these two points, where only the particle sizes differ from each other and the experimental conditions (SO_2 concentration, reaction time, stoichiometric ratio, reaction temperature, kind of sorbent, and injection method) are the same. The calculation includes the following steps:

(1) By applying the experimental data concerning the relationship between lime conversion (f) and particle radius (r) at the two points to Eq. 24, m_2 is calculated. This is denoted as m_2 ①.

(2) By applying the experimental values of f and r and an assumed value of R/r to Eq. 29, a value of m_2 for each experimental point is obtained. Subsequently, the m_2 values for the two points are averaged to yield m_2 ②.

(3) By applying the experimental value of f and r to Eq. 28, a value of m_2 for each experimental point is obtained for a state where primary particles are assumed. The values of m_2 for the two points are then averaged to yield m_2 ③.

(4) By applying experimental values of f and r and an assumed value of R/r to Eqs. 17 and 18, a value of $\bar{R}'$ is calculated. Subsequently, m_2 for imaginary primary particles is obtained from the (f, $\bar{R}'$) values for the two points, using the method described in step 1. The thus-obtained value is denoted as m_2 ④.

(5) The m_2 ① and m_2 ② indicate the m_2 value for the aggregate state, while the m_2 ③ and m_3 ④ are the m_2 values for the assumed primary particle state. In order to maintain the self-consistency of the present theory during the calculation of the m_2 values, the two m_2 values within each pair (one for the aggregate state and the other for the primary particle state) must be equal to each other. Therefore, through calculation of the m_2 ② value and the m_2 ④ value under the conditions where m_2 ② = m_2 ① and m_2 ③ = m_2 ④, the two assumed R/r values at the two experimental

points are simultaneously determined. For the calculation of Eqs. 17, 18, 28, and 29, the physicochemical constants designated in the previous section ($D_e = 10^{-7}$ m^2·s^{-1}, $D_m = 10^{-4}$ m^2·s^{-1}, and $k_c = 5$m·s^{-1}) were used.

An example of these 5 steps of the calculation will be shown below.

According to the experimental data shown in Figure 6, the value of η ($= f$) at an SR of 1 is 0.42 when $\bar{d}_{50} = 1$ μm and 0.25 when $\bar{d}_{50} = 1$ μm. From the experimental data at these two points, the degree of aggregation at a $\bar{d}_{50}$ of 1 and 5μm can be calculated as follows. First, m_2 ① and m_2 ③ are obtained using steps 1 and 3.

$$m_2\,① = -\frac{\log f_2 - \log f_1}{\log r_2 - \log r_1} = -\frac{\log 0.25/0.42}{\log 5/1} = 0.322$$

$$m_2\,③ = \frac{0.7181 + 0.8516}{2} = 0.781$$

Then, through repeated trial and error, a value of R/r at $\bar{d}_{50} = 1$ μm and its value at $\bar{d}_{50} = 5$ μm, which satisfy both m_2 ② = 0.322 and m_2 ④ = 0.781, can be determined.

When R/r is 10.7 at a $\bar{d}_{50}$ of 1 μm, m_2 is calculated as 0.015 using Eq. 29, and $\bar{R}'/r$ and $\bar{R}'$ are calculated as 5.28 and as 2.64 μm, respectively, using Eqs. 17 and 18.

When R/r is 3.2 at a $\bar{d}_{50}$ of 5 μm, m_2 is calculated as 0.620 using Eq. 29, and $\bar{R}'/r$ and $\bar{R}'$ are calculated as 1.98 and 4.96 μm, respectively, using Eqs. 17 and 18.

Then, the following values can be obtained.

$$m_2\,② = \frac{0.015 + 0.620}{2} = 0.318$$

$$m_2\,④ = \frac{-\log 0.25/0.42}{\log 4.96/2.55} = 0.780$$

When the accuracy of the calculation of the R/r value was expressed as a standard deviation (σ) of the subtraction of the m_2 ②/m_2 ① and m_2 ④, m_2 ③ from 1, σ was equal to 0.009.

Therefore, the degree of aggregation (R/r) is estimated at 10.7 when $\bar{d}_{50} = 1$ μm and at 3.2 when $\bar{d}_{50} = 5$ μm.

Figure 5 shows the relationship between $\bar{d}_{50}$ and R/r calculated for the hexagonal closest packing and the random packing, by applying Ishihara et al.'s experimental data to the previously mentioned five steps of calculation. Every σ value calculated for these R/r values was 0.059 or less. Thus, the calculation was satisfactorily accurate.

Usually, powders change their physical properties greatly as their size exceeds or becomes smaller than 5 μm. As powders become smaller than 2–3 μm, their attraction force is said to increase sharply.

Takada and Fukushima (1977) studied the relationship between the physical properties of talc powders and their particle sizes, and reported a relationship similar to the one observed between $\bar{d}_{50}$ and the degree of aggregation in the present study (Figure 5). This finding of Takada and Fukushima endorses the validity of the present theoretical equations. In an aerosol system produced by an ordinary

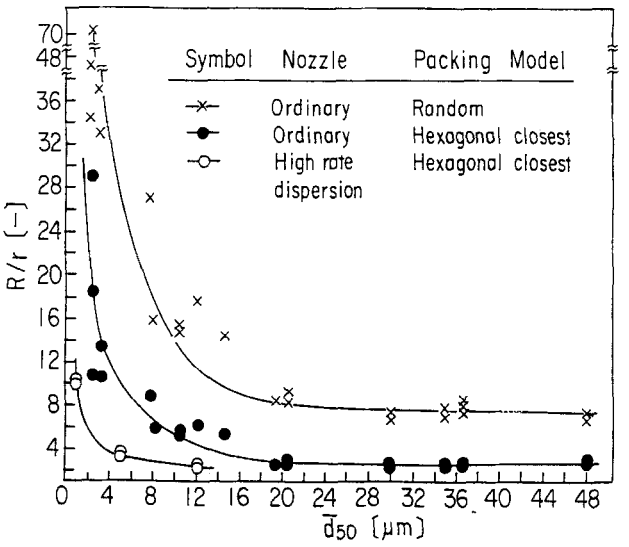

Figure 5. Relationship between mean particle diameter ($\bar{d}_{50}$) and degree of aggregation (R/r) calculated from experimental data concerning effect of particle size on aerosol SO_x removal.

method of injection, it is generally thought that the degree of aggregation (R/r) is smaller than 20–30 at a $\bar{d}_{50}$ value of 2–3 μm, and is approximately equal to 1 when $\bar{d}_{50}$ is larger than 40–50 μm. In the case of random packing, however, the R/r values calculated tend to be higher than their ordinary values and vary greatly among different experiments. This tendency is more marked when the mean particle diameter ($\bar{d}_{50}$) and the packing fractions (α and β), as described in the first section, decrease. Also in the case of the hexagonal closest packing, the R/r value was between 2 and 3 at a $\bar{d}_{50}$ of 40–50 μm, somewhat higher than the just-mentioned R/r value close to 1. This phenomenon may be interpreted as indicat-

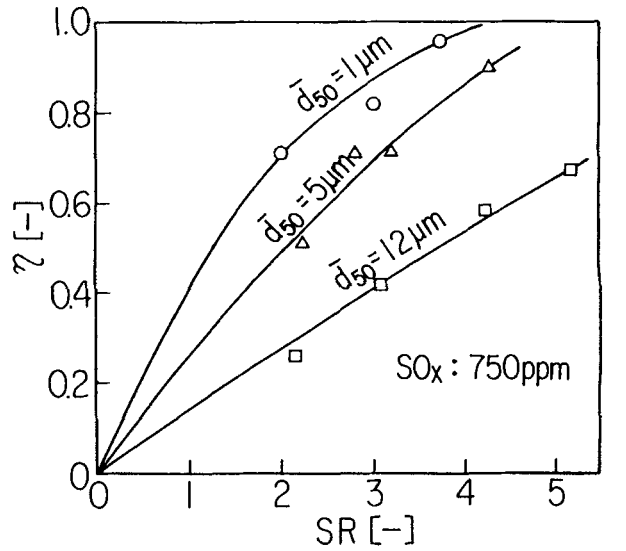

Figure 6. Experimental data by using high rate dispersion nozzle concerning effect of particle size on SO_x removal.

ing that the packing fractions become higher than those for the hexagonal closest packing model, since finer particles fill the spaces within the closest packing structure.

Aerosol reaction experiment by using a high-rate dispersion nozzle

Miura and Ogino (1985) used a high-rate dispersion nozzle to facilitate the dispersion of limestone powder, when they carried out some desulfurizing experiments that involved the injection of the fine limestone powder into furnaces. The nozzle they used was manufactured on the basis of the study carried out by Suganuma and Yamamoto (1983). The nozzle is an orifice-type nozzle, 6 mm in diameter and with 8 holes. Through this nozzle, air filled with dust at a concentration of 100 $g \cdot m^{-3}$ was squirted at a high rate (about 200 $m \cdot s^{-1}$).

Figure 6 shows the data of the experiments in which Tohjo's limestone powder with 3 particle sizes ($\bar{d}_{50} = 1$, 5, and 12.1 μm) were squirted into combustion gas that was 750 ppm in SO_2 concentration, about 1,100°C at temperature and about 1,500 $Nm^3 \cdot h^{-1}$ in gas capacity.

Figure 5 shows the results of the calculation on the basis of the experimental data shown in Figure 6, using the method described in the previous section. The standard deviation (σ), indicating the accuracy of calculation mentioned in that section, was always below 0.026. When the analytical results for the ordinary injection nozzle of Ishihara et al. are compared with the analytical results for the high-rate dispersion nozzle (Figures 4 and 6), the degree of aggregation for the high-rate dispersion nozzle is smaller than that for the ordinary nozzle, endorsing the efficacy of the high-rate dispersion nozzle. This result demonstrates that the efficiency of SO_x removal can be elevated by modifying the injection nozzle. Complete dispersion of the powder was not achieved in any of these analyses as shown in Figures 4 and 5. This does not represent a defect of the present theory or the analytical method. Instead, it can be attributed to the large difference in the concentration of the powder loaded on the dispersion nozzle between the present experiment (about 100 $g \cdot m^{-3}$) and the experiment carried out by Suganuma and Yamamoto in 1983 (below 10 $g \cdot m^{-3}$). That is, the orifice-type nozzle, whose powder loading capacity is relatively small, did not allow adequate dispersion of powder.

Stationary reaction experiment by using a thermobalance

Hasatani et al. (1982) studied the reactivity of limestone of varying particle sizes (5 μm) with SO_2, by means of a thermobalance experiment using 10–15-mg samples. They found that (1) the chronological weight changes suggested the predominance of chemical reactions processes; (2) the activation energy, as estimated from the temperature dependency of weight changes, was 27 kJ/mol; and (3) 450 s were required to obtain a lime conversion (f) of 0.12 when the SO_2 concentration was 3,700 ppm. The activation energy of 27 kJ/mol is a reasonable value, if diffusion rather than chemical reactions is controlling. Furthermore, in the aerosol reaction experiments, carried out by Ishihara et al. (1968, 1970, 1975), using 10-μm limestone powder in the presence of 2,390 ppm SO_2, an f value of 0.12 was obtained in 0.2–0.3 s, which differs by three or more orders of magnitude from the reaction time of 450 s reported by Hasatani et al.

Table 2. Contributions of Controlling Steps and $\bar{R}'/r$ Value Estimated Based on the Random Packing Model and on the Data from the Thermobalance Experiment of Hasatani et al.

$\bar{d}_{50}$ (μm)	α	β	R/r	AF_1/F_0 (%)	F_2/F_0 (%)	$(D_e/k_c \cdot r)F_3/F_0$ (%)	$\bar{R}'/r$
5	0.20	0.42	655.7	99.8	0.2	0.01	112
58	0.35	0.55	46.9	83.0	17.0	0.01	8.8

Based on these results, it may be said that the reaction experiments using a thermobalance are controlled by the apparent gas layer diffusion due to aggregation, rather than by chemical reactions, as suggested by Hasatani et al.

To test the validity of this view, the author calculated the $\bar{R}'/r$ values and the percent contribution of each process, by applying the experimental data, obtained at $\bar{d}_{50} = 5$ μm or 58 μm to Eqs. 17, 18, and 19, thereby regarding the 10-mg thermobalance sample as a randomly packed aggregate. This calculation was done under the conditions where $D_e = 10^{-7}$ $m^2 \cdot s^{-1}$; $D_m = 10^{-4}$ $m^2 \cdot s^{-1}$; $k_c = 5 m \cdot s^{-1}$; $f = 0.9$; and $SR = 0.001$ (great excess of SO_2 = stationary reaction). Packing fractions (α and β) were determined as shown in Figures 2 and 3. The R/r value was calculated from the number (n) of particles constituting 10-mg powder and from Eq. 1. The results are shown in Table 2.

The calculation reveals that 5-μm particles behave as a single particle of the size of 560 μm ($= 112 \times 5$ μm) in this reaction system. This means that the apparent gas layer diffusion (diffusion within the aggregate) process completely controls the reaction. Also in the reaction system of 58-μm particles, the particles behave like a single particle of the size of 510 μm ($= 8.8 \times 58$ μm), indicating that the apparent gas layer diffusion (diffusion within the aggregate) process controls 86% of the reaction.

These results of the calculation agree with the view that thermobalance reaction systems are controlled by the gas layer diffusion due to aggregation, rather than by chemical reactions.

Simulation Using the Theoretical Equations

To represent in concrete terms the concepts deduced in the first section (concepts of the reaction-equivalent radius, the effective reaction-equivalent radius, the acid gas concentration exponent, and the particle radius exponent), the author carried out a simulation of the behavior of 1-μm particles, using the hexagonal closest packing model whose validity was demonstrated in the third section, and using physicochemical constants in the second section ($D_e = 10^{-7}$ $m^2 \cdot s^{-1}$, $D_m = 10^{-4}$ $m^2 \cdot s^{-1}$, and $k_c = 5$ $m \cdot s^{-1}$). Figure 7 shows the results of the calculations, using Eqs. 17 and 18.

In early phases of reactions, the layer of reaction products is not thick and the resistance to diffusion within the reaction product layer is small, resulting in a relatively larger resistance to diffusion in the apparent gas layer (diffusion within the aggregate). For this reason, the aggregate's R'/r is close to R/r in the early phases of reactions, but it becomes smaller than R/r in advanced phases of reactions. At an ordinary lime conversion (approximately equal to 0.2), the R'/r is approximately 40–45% of the R/r, and the $\bar{R}'/r$ is approximately 50–70% of the R/r. These results indicate that the

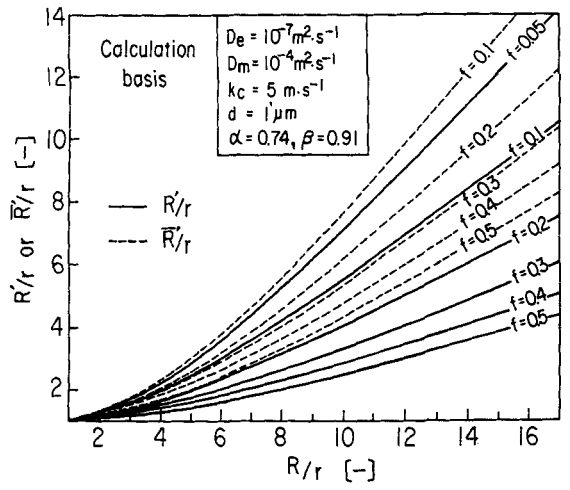

Figure 7. Simulation of relationship among effective reaction-equivalent radius ratio ($\bar{R}'/r$), reaction-equivalent radius ratio (R'/r), degree of aggregate (R/r), and lime conversion (f) in aggregate reaction system.

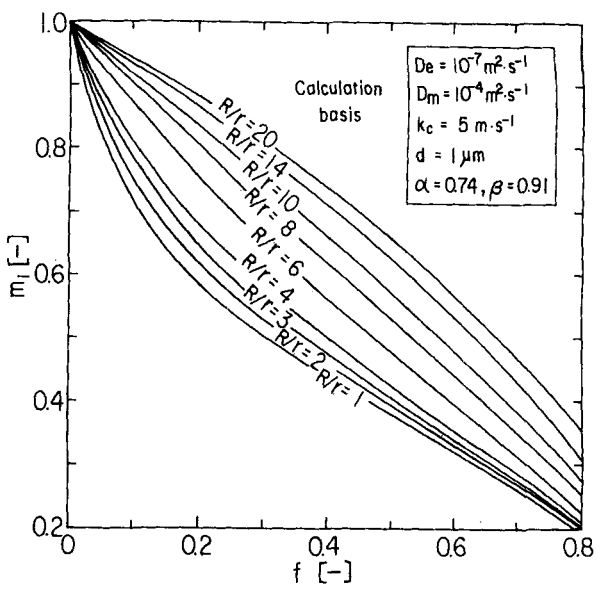

Figure 8. Simulation of relationship among SO_x gas concentration exponent (m_1), lime conversion (f), and degree of aggregate (R/r).

aggregate is more reactive than the primary particles of the same size.

Figure 8 shows the results of calculations using Eqs. 22 and 23. Figure 9 shows the results of calculations using Eqs. 28 and 29. As is noticeable in these figures, the m_1 value increased as the degree of aggregation became higher, while the m_2 value decreased sharply as aggregation became more intense. The tendency for the m_2 value to decrease sharply following intensification of aggregation provides a good explanation of the phenomenon that the particle-size dependency (m_2 value) is low during dry flue-gas desulfurization.

Conclusion

Using the theoretical equations concerning powder/gas reaction, based on the particle packing models, the author carried out some analyses and simulations by applying experimental data to these equations. The following results were obtained:

(1) The curves indicating the relationship between the mean particle size ($\bar{d}_{50}$) and the degree of aggregation (R/r) and that between ($\bar{d}_{50}$) and the effective diffusivity in reaction product layer (D_e), as determined from the analyses of the data concerning the effects of particle sizes in aerosol reactions, agreed well with the aggregating characteristics of powders. This finding endorses the validity of the theory presented.

(2) When the effects of particle sizes on aerosol reactions were examined, using two packing models (hexagonal closest packing and random packing), the hexagonal closest packing model was found to represent the aggregation characteristics of aerosols more faithfully.

(3) The use of a high-rate dispersion nozzle was found to reduce the degree of aggregation in the aerosol and consequently to elevate the reaction efficiency.

(4) The thermobalance experiment of the reactions between 10 mg of limestone powder and SO_2, revealed that the percent contribution of gas layer diffusion (diffusion within the aggregate) to the overall reaction rate equation was estimated to be 99.8% for 5-μm limestone powder and 83.0% for 58-μm limestone powder. It is suggested that bulk limestone powder behaves as if it were a giant primary particle of a size equivalent to 560 μm (in the case of 5-μm powder) and 510 μm (in the case of 58-μm powder.

(5) Graphic representation of the relationships among R/r (degree of aggregation), R'/r (reaction-equivalent radius ratio), and $\bar{R}'/r$ (effective reaction-equivalent radius ratio) revealed that the order of magnitude of these three values was $R/r > \bar{R}'/r > R'/r$ and that the aggregate was considerably more reactive than the primary particles of the same size.

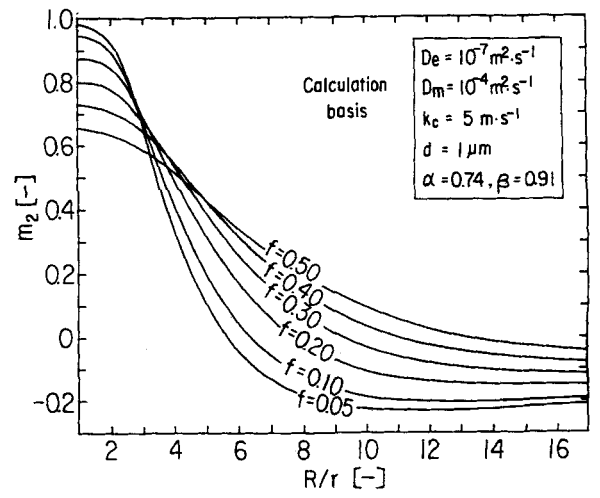

Figure 9. Simulation of relationships among particle radius exponent (m_2), degree of aggregate (R/r), and line conversion (f).

(6) Graphic representation of the relationship between the m_2 value (particle-size exponent) and R/r (degree of aggregation) revealed that the particle-size dependency of the lime conversion decreased sharply as the degree of aggregation became higher.

Acknowledgment

The author is indebted to Prof. Emeritus Tatsuo Tanaka, Hokkaido University, for the valuable advice he provided during the course of this study.

Notation

a = micropore radius of intraparticle, m
C_s = concentration of gas at external surface, $mol \cdot m^{-3}$
C_f = concentration of gas in bulk phase, $mol \cdot m^{-3}$
d = particle diameter, m
F = dimensionless resistance of reaction steps
F_0 = overall
F_1 = gas layer diffusion controlling
F_2 = reaction product layer diffusion controlling
F_3 = chemical reaction controlling
K_f = mass-transfer coefficient in gas layer of aggregate, $m \cdot s^{-1}$
k_f = mass-transfer coefficient in gas layer of primary particle, $m \cdot s^{-1}$
k'_f = apparent mass-transfer coefficient in gas layer of primary particles within aggregate, $m \cdot s^{-1}$
k'_{f_0} = surface of aggregate
k'_{f_1} = intraaggregate
M = molecular weight, $kg \cdot mol^{-1}$

Literature Cited

Borgwardt, R. H., "Calcination Kinetics and Surface Area of Dispersed Limestone Particles," *AIChE J.*, **31**, 103 (1985).
Borgwardt, R. H., and K. R. Bruce, "Effect of Specific Surface Area on the Reactivity of CaO with SO_2," *AIChE J.*, **32**, 239 (1986).
Borgwardt, R. H., K. R. Bruce and N. F. Roache, "Method for Variation of Grain Size in Studies of Gas-Solid Reactions Involving CaO," *Ind. Eng. Chem. Fund.*, **25**, 165 (1986).
Borgwardt, R. H., "Sintering of Nascent Calcium Oxide," *Chem. Eng. Sci.*, **44**, 53 (1989a).
Borgwardt, R. H., "Calcium Oxide Sintering in Atmospheres Containing Water and Carbon Dioxide," *Ind. Eng. Chem. Res.*, **28**, 493 (1989b).
Gilliland, R. E., "Diffusion Coefficients in Gaseous System," *Ind. Eng. Chem.*, **26**, 681 (1934).
Gotoh, K., "Random Structure of Particle Assemblies and Physicochemical Properties of Liquids," *Advances in The Mechanics and The Flow of Granular Materials*, Vol. 1, Gulf Publishing, p. 41 (1983).
Hasatani, M., M. Yusawa, and N. Arai, "Reactivity of CaO Produced by Pyrolysis of Micro-Fine Limestone Particle with SO_2," *Kagaku-Kogaku-Ronbunshu*, **8**, 45 (1982).
Ishihara, Y., C. Asakawa, and H. Hukuzawa, "Pilot Furnace Experiments on Removing Sulfur Dioxide from Combustion Gas by Limestone Injection Method," *Denryoku-Chuo-Kenkyusho Hokoku*, No. 67057 (1967).
Ishihara, Y., C. Asakawa, and H. Hukuzawa, "Removal of Sulfur Dioxide from Flue Gases by Limestone, by Hydrated Lime or Dolomite," *Denryoku-Chuo-Kenkyusho Hokoku*, No. 68024 (1968).
Ishihara, Y., and H. Hukuzawa, "Kinetics of the Reaction of Calcined Limestone with Sulfur Dioxide in Combustion Gases," *Denryoku-Chuo-Kenkyusho Hokoku*, No. 70006 (1970).
Ishihara, Y., C. Asakawa, and H. Hukuzawa, "Studies on Sulfur Oxides Removal from Flue Gas by Dry Limestone Injection Process: II. Effects of Reaction Conditions on Sulfur Oxides," *Nenryo-Kyokai-Shi*, **54**, 175 (1975).
Ishihara, Y., and H. Hukuzawa, "Studies on Sulfur Oxides Removal from Flue Gas by Dry Limestone Injection Process: III. Discussion on the Effect of Factors Affecting the Reaction Rate of Sulfur Dioxide with Limestone Particles Injected into Combustion Gas," *Nenryo-Kyokai-Shi*, **54**, 321 (1975a).
Ishihara, Y., and H. Hukuzawa, "Studies on Sulfur Oxides Removal from Flue Gas by Dry Limestone Injection Process: IV. An Analysis of Mass Transfer in the Reaction of Sulfur Dioxide with Calcined Limestone Particles in Combustion Gases," *Nenryo-Kyokai-Shi*, **54**, 923 (1975b).
Kobayashi, Y., "Theoretical Studies of Acid Gas Removal by Lime/Limestone Powder Injection," *Kagaku-Kogaku Ronbunshu*, **19**, 840 (1993).
Miura, Y., and E. Ogino, Technical Data of Hitachi-Zosen, unpublished (1985).
Nitto, F. K., *Catalogue of Limestone Powder*, Tsukuda 7-Chome, Osaka (1990).
Suganuma, A., and H. Yamamoto, "Dispersion of Aggregated Airborne Dust by Orifice," *Kagaku-Kogaku Ronbunshu*, **9**, 183 (1983).
Takada, S., and S. Fukushima, "Effects of Particle Size on Physical Properties of Talc," Colloquium in Tokai Branch of Soc. of Chem. Eng. Japan, Nagoya, p. 45 (1977).
Wickert, K., "Versuche zur Entschwefelung vor und hinter dem Brenner zur Verringerung des SO_2-Auswurfs," VGB **83** 74 (1963).

Appendix A: Mass-Transfer Coefficient in the Gas Layer of Particles in an Aerosol

Assuming a quasi-steady state in which the particle radius is denoted as R, the radius of the particle-occupied space as $L/2$, and the distance from the particle center as x, the gas transfer rate from the particle-occupied space to the particle surface can be expressed by Eq. A1.

$$4\pi X^2 D_m \frac{dC}{dX} = 4\pi R^2 k_f (C_f - C_s) \tag{A1}$$

Integrating the left side of Eq. A1 from the margin of the particle-occupied space ($x = L/2$, $C = C_f$) through the particle surface ($x = R$, $C = C_s$), Eq. A2 can be obtained:

$$\text{Left side of Eq. A1} = 4\pi D_m \cdot \frac{R}{1-2R/L} \cdot (C_f - C_s) \tag{A2}$$

From Eqs. A1 to A3 can be obtained:

$$k_f = \frac{D_m}{R(1-2R/L)} \tag{A3}$$

Manuscript received July 5, 1994, and revision received Nov. 7, 1994.